Calculation of multiphoton-ionization Green's functions using the Wentzel-Kramers-Brillouin approximation

Mark Edwards
Department of Physics, Georgia Southern University, Statesboro, Georgia 30460
(Received 17 May 1991; revised manuscript received 15 August 1991)

We present a uniform method for approximating the functions that appear in the N-photon radial matrix element. This matrix element is required for calculating multiphoton-ionization cross sections and angular distributions in lowest-order perturbation theory. The functions include the initial- and final-state radial wave functions, and the regular and irregular parts of the radial Green's function. We point out that all of these functions satisfy a differential equation of the same form, and differ only in their boundary conditions. The WKB method is then applied to this differential equation to obtain approximations to all of these functions. We then use these solutions to calculate two-photon-ionization cross sections of hydrogen for photon energies between 8.5 and 13.2 eV. Also presented are two-photon-ionization cross sections for Cs around the minimum near the $7p$ resonance and comparisons with previous work.

PACS number(s): 32.80.Rm, 42.50.Hz

I. INTRODUCTION

Over the past decade, experimental techniques for measuring multiphoton-ionization cross sections and angular distributions have outstripped the capability of known theoretical techniques for calculating them. A case in point is the existence of experimental data [1] on the above-threshold ionization of Xe. As far as this author is aware, there has been no attempt to calculate the cross section or angular distribution for this case in lowest-order perturbation theory.

There are two major difficulties in performing these calculations. First, accurate atomic wave functions are required; and second, a method for performing the infinite summations over the complete set of atomic states (both bound and continuum) is needed. Many of the methods used in the past have balanced these two requirements.

Methods for evaluating the summation have included the truncated-summation method [2], the Dalgarno-Lewis technique [3], and the Green's-function method [4]. In the truncated summation technique, the infinite sums are approximated with finite sums which are evaluated with accurate wave functions. These wave functions have recently been calculated using quantum-defect theory and also using a finite L^2 basis [5,6] constructed with B splines. The generalized Dalgarno-Lewis method involves conversion of the summation into a system of coupled differential equations which are then solved numerically.

In the Green's-function method, the summation is converted to an N-dimensional integral with the Green's functions replacing the infinite summations. The technique consists of first evaluating the Green's function and then evaluating the integral. A numerical technique for evaluating the integral has been reported previously [7]. It is with the evaluation of the Green's functions that this paper is concerned.

In Sec. II, we present the N-photon matrix element and point out that the functions in the integrand of this matrix element (the radial parts of the initial bound-state wave function, the regular and irregular parts of the radial Green's function, and the final continuum state), all satisfy a differential equation of the same form, but have different boundary conditions. In Sec. III, we transform this differential equation into a form which is similar to the Schrödinger wave equation for a particle moving in a one-dimensional potential. The well-known WKB approximation general solution can then be immediately written down and the inverse transformation performed. This method of applying the WKB approximation was first proposed by Langer [8] and elaborated upon by others [9]. We then derive the continuum- and bound-state wave functions and the regular and irregular parts of the Green's function by applying the boundary conditions to these general WKB solutions.

The WKB general solution has different forms for different intervals of the radial coordinate. The end points of these intervals are roughly determined by the positions of the turning points of the classical motion of the electron. The WKB solutions in regions far from the turning points are termed "proper solutions" and these solutions diverge at the turning points. Solutions valid near a turning point are called "local solutions."

In Sec. IV we outline the method for determining the precise locations of the regions of validity for each piece of the whole solution. We also show where these regions are located as a function of photon energy for the cross-section results presented in Sec. V. In Sec. V we use these approximate Green's functions and wave functions to calculate the two-photon-ionization cross section for photon energies ranging from 8.5 to 13.2 eV. In addition, we present calculated two-photon-ionization cross sections for Cs around the minimum near the $7p$ resonance and compare with previous work.

Finally, in Sec. VI we discuss the importance of the

atomic potential in regard to the performance of the method and present the model potential used in the Cs cross-section calculation.

II. N-PHOTON RADIAL MATRIX ELEMENT

The fundamental quantity needed to calculate the generalized multiphoton-ionization cross section or angular distribution in lowest-order perturbation theory is [7]

$$M^{(N)}_{\nu_N\cdots\nu_0}=\int_0^\infty dr_N\cdots\int_0^\infty dr_1 u_{\nu_N}(r_N) \times r_N g_{\nu_{N-1}}(r_N,r_{N-1}) \times\cdots r_1 u_{\nu_0}(r_1)\ , \quad (2.1)$$

where $\nu_n=(E_n,l_n)$, $E_n=E_0+n\hbar\omega$, (E_0 is the energy of the initial atomic state and ω is the laser photon frequency), and l_n is the angular momentum of the set of intermediate states reached by the absorption of n photons. In the above equation, the quantities $u_{\nu_N}(r)$ and $u_{\nu_0}(r)$ are the radial parts of the final continuum- and initial-state wave functions, respectively. The factor $g_\nu(r,r')$ is the radial Green's function which satisfies the following equation:

$$(E-H_\nu)g_\nu(r,r')=\delta(r-r'),\quad \nu=(E,l) \quad (2.2)$$

where

$$H_\nu=-\frac{1}{2}\frac{d^2}{dr^2}+\tfrac{1}{2}l(l+1)r^{-2}+U(r)\ . \quad (2.3)$$

We use atomic units throughout the rest of this paper. The function $U(r)$ is the full potential seen by the electron. The solution of (2.2) can be written as [7]

$$g_\nu(r,r')=-2\pi R_\nu(r_<)I_\nu(r_>)\ , \quad (2.4)$$

where $r_<$ and $r_>$ are the lesser and greater of r and r', respectively, and $R_\nu(r)$ and $I_\nu(r)$ are, respectively, the regular and irregular solutions of the homogeneous form of Eq. (2.2)

$$(E-H_\nu)\psi_\nu=0\ . \quad (2.5)$$

The continuum- and bound-state wave functions also satisfy this equation for different values of E and l, thus all of the functions in the integrand of Eq. (2.1) (aside from factors of r) satisfy a differential equation of the same form. The only difference between them is the imposed boundary conditions.

The boundary conditions for the functions $u_{\nu_N}(r)$, $u_{\nu_0}(r)$, $R_\nu(r)$, and $I_\nu(r)$ are as follows:

$$u_{\nu_N}(0)=0\ . \quad (2.6a)$$

$$u_{\nu_N}(r)\underset{r\sim\infty}{\sim}(2/\pi)^{1/2}k^{-1/2}\sin(\theta_{\nu_N}+\delta_{\nu_N})\ , \quad (2.6b)$$

$$R_\nu(0)=0\ , \quad (2.7a)$$

$$R_\nu(r)\underset{r\sim\infty}{\sim}(2/\pi)^{1/2}k^{-1/2}\sin(\theta_\nu+\delta_\nu)\ , \quad (2.7b)$$

$$I_\nu(r)\underset{r\sim 0}{\sim}D_\nu r^{-l}\ , \quad (2.8a)$$

$$I_\nu(r)\underset{r\sim\infty}{\sim}\tfrac{1}{2}(2/\pi)^{1/2}k^{-1/2}\exp[i(\theta_\nu+\delta_\nu)]\ , \quad (2.8b)$$

$$u_{\nu_0}(0)=0\ , \quad (2.9a)$$

$$u_{\nu_0}(\infty)=0\ , \quad (2.9b)$$

where

$$k=(2E)^{1/2}\ . \quad (2.10a)$$

We draw a branch cut along the positive energy axis and take the branch of the square root which is positive when E is on the upper side of this cut. Also,

$$\theta_\nu=kr-\tfrac{1}{2}l\pi+(1/k)\ln(2kr)+\eta_\nu \quad (2.10b)$$

and

$$\eta_\nu=\arg[\Gamma(l+1-i/k)]\ . \quad (2.10c)$$

D_ν is a constant. The symbol η_ν is the Coulomb phase shift and δ_ν is the part of the total phase shift due to the non-Coulomb part of the potential $U(r)$. The fact that all of these functions satisfy Eq. (2.5) allows us to develop a unified method for approximating all of them based on the WKB method. Quantities such as WKB atomic energy levels and phase shifts are also approximated using this method. We present this method below.

III. WKB GREEN'S FUNCTIONS AND WAVE FUNCTIONS

A. WKB general solution

The application of the WKB approximation to Eq. (2.5) separates naturally into two parts depending on whether E is greater than or less than zero. In this article we shall not consider above-threshold ionization processes, therefore only the final continuum-state wave function must be evaluated for $E>0$.

The first step in applying the WKB method [9] is to transform the independent variable (r) and the dependent variable (ψ_ν) in Eq. (2.5) as follows:

$$r=e^x \quad (3.1)$$

and

$$\psi_\nu=e^{(1/2)x}\phi_\nu(x)\ . \quad (3.2)$$

Transformation (3.1) has the effect of stretching the domain of the independent variable from $r\in[0,+\infty)$ to $x\in(-\infty,+\infty)$. Application of this transformation yields a differential equation containing a first-derivative term which is unsuitable for applying the WKB approximation. Subsequent application of transformation (3.2) removes this term and gives the following equation for $\phi_\nu(x)$:

$$\phi_\nu''(x)+2e^{2x}[E-U_{\text{eff}}(x)]\phi_\nu(x)=0, \quad (3.3a)$$

where

$$U_{\text{eff}}(x)=U(e^x)+\tfrac{1}{2}(l+\tfrac{1}{2})^2e^{-2x}\ . \quad (3.3b)$$

Equation (3.3a) bears a formal resemblance to the

Schrödinger wave equation for a particle moving in a one-dimensional potential. All of the well-known WKB solutions for that equation may be applied to Eq. (3.3). This method of applying the WKB method to the radial wave equation was first introduced by Langer [8]. Note that a small, but significant, change has been produced by transformations (3.1) and (3.2). The term $l(l+1)r^{-2}$ has become $(l+\frac{1}{2})^2 e^{-2x}$ and does not vanish when $l=0$.

The second step is to write down the WKB general solutions for Eq. (3.3). The form of these solutions differs according to the sign of the coefficient multiplying $\phi_\nu(x)$ in that equation. Figure 1 shows a typical plot of $U_{\text{eff}}(x)$ along with horizontal lines depicting two values of E, one greater than and one less than zero.

The points at which the line $E=$const and $U_{\text{eff}}(x)$ intersect are the classical turning points and are also the points around which the proper WKB solutions fail. For $E>0$, in the interval $(-\infty, x_0')$, (labeled region I in Fig. 1), the coefficient of $\phi_\nu(x)$ in Eq. (3.3) is less than zero. In the interval $(x_0', +\infty)$ (labeled region II), this coefficient is greater than zero. Also, in a small region around x_0' (region A), the proper WKB solution fails and a local solution is appropriate. Thus, for $E>0$, the full solution divides into three pieces which must be joined so that the entire approximate function is continuous.

For $E<0$, there are two turning points which divide the x axis into five regions: region I $(-\infty, x_0)$; region II (x_0, x_1); region III $(x_1, +\infty)$, and two local regions around x_0 (region A) and around x_1 (region B). See Fig. 1.

The general WKB solutions of Eq. (3.3a) are [9], for $E>0$,

$$\phi_\nu^{(I)}(x)=|q_\nu(x)|^{-1/2}\{A_I\exp[-|w_\nu(x)|] + B_I\exp[+|w_\nu(x)|]\}\ , \tag{3.4a}$$

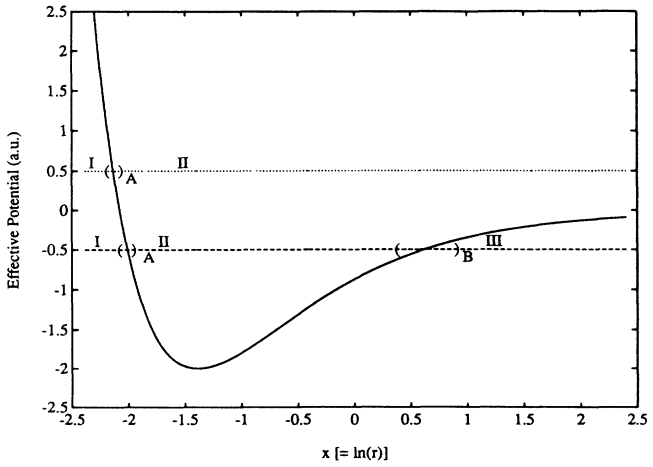

FIG. 1. A plot of the effective potential for hydrogen with $l=0$ which identifies the regions associated with the different parts of the WKB general solutions. The parentheses indicate the local regions around the turning points and are labeled with letters, while regions far from the turning points are labeled with roman numerals.

$$\phi_\nu^{(A)}(x)=[w_\nu(x)/q_\nu(x)]^{1/2}[AJ_{+1/3}(w_\nu(x)) + BJ_{-1/3}(w_\nu(x))]\ , \tag{3.4b}$$

$$\phi_\nu^{(II)}(x)=[q_\nu(x)]^{-1/2}\{A_{II}\exp[+iw_\nu(x)] + B_{II}\exp[-iw_\nu(x)]\}\ , \tag{3.4c}$$

where

$$q_\nu^2(x)=2e^{2x}[E-U_{\text{eff}}(x)] \tag{3.4d}$$

and

$$w_\nu(x)=\int_{x_0}^{x} q_\nu(x')dx'\ . \tag{3.4e}$$

In Eq. (3.4b), $J_{\pm 1/3}(y)$ are Bessel functions of order $\pm\frac{1}{3}$. Extreme care must be exercised in taking the proper branch of the square root of $q_\nu^2(x)$ and when taking the modulus of $w_\nu(x)$ especially when evaluating Eq. (3.4b).

The function $w_\nu(x)$ is defined so that it increases as x moves away from the turning point. In order to ensure the continuity of the final solution we shall need the asymptotic forms of Eq. (3.4b) for $x \ll x_0$ and $x \gg x_0$, respectively,

$$\phi_\nu^{(A)}(x)\sim \tfrac{1}{2}(2/\pi)^{1/2}|q_\nu(x)|^{-1/2} \times\{(B-A)\exp[+|w_\nu(x)|] + (Ae^{i\pi/6}+Be^{-i\pi/6})\exp[-|w_\nu(x)|]\}\ , \tag{3.5a}$$

$$\phi_\nu^{(A)}(x)\sim \tfrac{1}{2}(2/\pi)^{1/2}[q_\nu(x)]^{-1/2} \times\{e^{-i\pi/4}(Ae^{-i\pi/6}+Be^{i\pi/6})\exp[+iw_\nu(x)] + e^{i\pi/4}(Ae^{i\pi/6}+Be^{-i\pi/6})\exp[-iw_\nu(x)]\}\ . \tag{3.5b}$$

The second term in Eq. (3.5a) can be considered only if the first term vanishes, (i.e., B is exactly equal to A), because of the dominance of the increasing exponential in the asymptotic form.

The WKB solution has the following form for $E<0$:

$$\phi_\nu^{(I)}(x)=|q_\nu(x)|^{-1/2}\{A_I\exp[-|w_\nu(x)|] + B_I\exp[+|w_\nu(x)|]\}\ , \tag{3.6a}$$

$$\phi_\nu^{A}(x)=[w_\nu(x)/q_\nu(x)]^{1/2}[AJ_{+1/3}(w_\nu(x)) + BJ_{-1/3}(w_\nu(x))]\ , \tag{3.6b}$$

$$\phi_\nu^{(II)}(x)=[q_\nu(x)]^{-1/2}\{A_{II}\exp[iw_\nu(x)] + B_{II}\exp[-iw_\nu(x)]\}\ . \tag{3.6c}$$

An alternate solution in region II useful for matching boundary conditions is

$$\phi_\nu^{(II)}(x)=[q_\nu(x)]^{-1/2}\{A_{II}e^{i\alpha_\nu}\exp[-iw_\nu'(x)] + B_{II}e^{-i\alpha_\nu}\exp[iw_\nu'(x)]\}\ , \tag{3.6d}$$

where

$$w'_\nu(x)=\int_x^{x_1} q_\nu(x')dx' \tag{3.6e}$$

and

$$\alpha_\nu=\int_{x_0}^{x_1} q_\nu(x')dx' \ . \tag{3.6f}$$

The solutions for regions B and III are

$$\phi_\nu^{(B)}(x)=[w'_\nu(x)/q_\nu(x)]^{1/2}[A'J_{+1/3}(w'_\nu(x))+B'J_{-1/3}(w'_\nu(x))] \ , \tag{3.6g}$$

$$\phi_\nu^{(III)}(x)=|q_\nu(x)|^{-1/2}\{A_{III}\exp[+|w'_\nu(x)|]+B_{III}\exp[-|w'_\nu(x)|]\} \ . \tag{3.6h}$$

The asymptotic behavior of $\phi_\nu^{(A)}(x)$ for $E<0$ is identical to Eqs. (3.5). The behavior of $\phi_\nu^{(B)}(x)$ for $x \ll x_1$ and $x \gg x_1$, respectively, is

$$\phi_\nu^{(B)}(x)\sim\tfrac{1}{2}(2/\pi)^{1/2}[q_\nu(x)]^{-1/2}\{e^{-i\pi/4}(A'e^{-i\pi/6}+B'e^{i\pi/6})\exp[iw'_\nu(x)]+e^{i\pi/4}(A'e^{i\pi/6}+B'e^{-i\pi/6})\exp[-iw'_\nu(x)]\} \ , \tag{3.7a}$$

$$\phi_\nu^{(B)}(x)\sim\tfrac{1}{2}(2/\pi)^{1/2}|q_\nu(x)|^{-1/2}\{(B'-A')\exp[+|w'_\nu(x)|]+(A'e^{i\pi/6}+B'e^{-i\pi/6})\exp[-|w'_\nu(x)|]\} \ . \tag{3.7b}$$

The last step is to determine the values of the coefficients in the above general solutions. This is done by applying continuity conditions in between the different parts of the solutions (internal boundary conditions), transforming them back to functions of r, and then imposing boundary conditions (2.6)–(2.9) at $r=0$ and ∞ (external boundary conditions).

B. Internal boundary conditions

For $E>0$, we guarantee continuity of the solutions by matching the coefficients of $\exp[\pm iw_\nu(x)]$ in $\phi_\nu^{(I)}(x)$ [Eq. (3.4a)], with those in the asymptotic form of $\phi_\nu^{(A)}(x)$ for $x \ll x_0$ [Eq. (3.5a)]. Similarly, we match the appropriate coefficients in $\phi_\nu^{(II)}(x)$ [Eq. (3.4c)] with those in the asymptotic form of $\phi_\nu^{(A)}(x)$ for $x \gg x_0$ [Eq. (3.5b)]. This yields the following system of linear equations for $E>0$:

$$A_I=\tfrac{1}{2}(2/\pi)^{1/2}(Ae^{i\pi/6}+Be^{-i\pi/6}), \tag{3.8a}$$

$$B_I=\tfrac{1}{2}(2/\pi)^{1/2}(B-A) \ , \tag{3.8b}$$

$$A_{II}=\tfrac{1}{2}(2/\pi)^{1/2}e^{-i\pi/4}(Ae^{-i\pi/6}+Be^{i\pi/6}) \ , \tag{3.8c}$$

$$B_{II}=\tfrac{1}{2}(2/\pi)^{1/2}e^{i\pi/4}(Ae^{i\pi/6}+Be^{-i\pi/6}) \ . \tag{3.8d}$$

For $E<0$ we match coefficients in the following pairs of equations: (3.6a) and (3.5a); (3.6c) and (3.5b); (3.6d) and (3.7a); and (3.6h) and (3.7b). This matching produces a linear system of eight equations, the first four of which are identical to Eqs. (3.8) and the remaining four are for $E<0$,

$$A_{II}e^{i\alpha_\nu}=\tfrac{1}{2}(2/\pi)^{1/2}e^{i\pi/4}(A'e^{i\pi/6}+B'e^{-i\pi/6}) \ , \tag{3.9a}$$

$$B_{II}e^{-i\alpha_\nu}=\tfrac{1}{2}(2/\pi)^{1/2}e^{-i\pi/4}(A'e^{-i\pi/6}+B'e^{i\pi/6}) \ , \tag{3.9b}$$

$$A_{III}=\tfrac{1}{2}(2/\pi)^{1/2}(B'-A') \ , \tag{3.9c}$$

$$B_{III}=\tfrac{1}{2}(2/\pi)^{1/2}(A'e^{i\pi/6}+B'e^{-i\pi/6}) \ . \tag{3.9d}$$

Note that Eq (3.8a) can only be used if $B=A$ and Eq. (3.9d) can only be used if $B'=A'$ due to the dominance of the increasing exponential in the asymptotic forms of the local solutions about the turning points.

To transform the solutions $\phi_\nu(x)$ back to the $\psi_\nu(r)$ we need only make the following replacements in Eqs. (3.4) and (3.6):

$$\phi_\nu \Longrightarrow \psi_\nu \ , \tag{3.10a}$$

$$q_\nu(x) \Longrightarrow C_\nu(r) \ , \tag{3.10b}$$

$$w_\nu(x) \Longrightarrow w_\nu(r) \ , \tag{3.10c}$$

and

$$w'_\nu(x) \Longrightarrow w'_\nu(r) \ , \tag{3.10d}$$

where

$$C_\nu^2(r)=2\{E-[U(r)+\tfrac{1}{2}(l+\tfrac{1}{2})^2r^{-2}]\} \ , \tag{3.11a}$$

$$w_\nu(r)=\int_{r_0}^{r} C_\nu(r')dr' \ , \tag{3.11b}$$

and

$$w'_\nu(r)=\int_{r}^{r_1} C_\nu(r')dr' \ . \tag{3.11c}$$

The positions of the turning points r_0 and r_1 are determined by

$$C_\nu^2(r_0)=0 \tag{3.12a}$$

and

$$C_\nu^2(r_1)=0 \ . \tag{3.12b}$$

C. WKB continuum state

To finally specify the Green's function and the continuum and bound states, we must impose the boundary conditions specified in Eqs. (2.6)–(2.9). We begin with the continuum-state wave function whose boundary conditions are given in Eqs. (2.6). Boundary condition (2.6a) forces the coefficient of the increasing exponential in Eq. (3.4a) (B_I) to be zero. This condition along with Eqs. (3.8) can be solved leaving one free parameter (A) in

which case $u_{\nu_N}(r)$ has the form

$$u_{\nu_N}^{(II)}(r)=2A(2/\pi)^{1/2}\cos(\pi/6)[C_\nu(r)]^{-1/2} \times\sin[w_\nu(r)+\pi/4] , \tag{3.13}$$

where we have also used Eqs. (3.4) and (3.10). Equating the asymptotic form of (3.13) with that given by boundary condition (2.6b), we can determine the value of the constant A and also the non-Coulomb part of the phase shift δ_{ν_N}. Since $[C_\nu(r)]^{-1/2}\sim k^{-1/2}$ as $r\sim+\infty$, it is clear that

$$A=[2\cos(\pi/6)]^{-1} . \tag{3.14}$$

A complete summary of the values of all constants determined by imposing boundary conditions may be found in Table I.

Specifying the phase shifts δ_{ν_N} and η_{ν_N} requires special consideration. We begin by rewriting Eq. (3.13) as follows:

$$u_{\nu_N}^{(II)}(r)=(2/\pi)^{1/2}[C_{\nu_N}(r)]^{-1/2} \times\sin\{w_{\nu_N}^{(c)}(r)+\pi/4+[w_{\nu_N}(r)-w_{\nu_N}^{(c)}(r)]\} , \tag{3.15}$$

where

$$w_{\nu_N}^{(c)}(r)=\int_{r_{0C}}^{r}\{2E_N-2[-(r')^{-1}+\tfrac{1}{2}(l_N+\tfrac{1}{2})^2r'^{-2}]\}^{1/2}dr' \tag{3.16a}$$

and

$$r_{0C}=\{[1+2E_N(l_N+\tfrac{1}{2})^2]^{1/2}-1\}/(2E_N) . \tag{3.16b}$$

The integral in Eq. (3.16a) can easily be evaluated. The asymptotic form of $w_\nu^{(c)}(r)$ for $E_N>0$ is

$$w_\nu^{(c)}(r)\underset{r\sim\infty}{\sim}k_Nr-\tfrac{1}{2}l_N\pi+(1/k_N) +(1/k_N)\ln(2k_N)+\eta_{\nu_N}^{(\mathrm{WKB})}-\pi/4 , \tag{3.17a}$$

where only terms small compared to π have been neglected and where

$$\eta_{\nu_N}^{(\mathrm{WKB})}=(1/k_N)-(1/k_N)\ln\{[(1/k_N)^2+(l_N+\tfrac{1}{2})^2]\} -(l_N+\tfrac{1}{2})\sin^{-1}\left[\frac{(1/k_N)}{[(1/k_N)^2+(l_N+\tfrac{1}{2})^2]^{1/2}}\right] \tag{3.17b}$$

is the WKB approximation to the Coulomb phase shift. It is important to compare $\eta_\nu^{(\mathrm{WKB})}$ to the exact expression given in Eq. (2.10c). We find that the error $\Delta\eta_\nu\equiv\eta_\nu-\eta_\nu^{(\mathrm{WKB})}$ is small compared to π for $E\geq0.2$ a.u. and that it is very weakly dependent on l.

The asymptotic form of Eq. (3.15) can then be written as

$$u_{\nu_N}^{(II)}\underset{r\sim\infty}{\sim}(2/\pi)^{1/2}k^{-1/2}\sin(\theta_{\nu_N}+\delta_{\nu_N}^{(\mathrm{WKB})}) , \tag{3.18}$$

where θ_{ν_N} is defined by Eq. (2.10b) and we identify the WKB non-Coulomb phase shift as

$$\delta_\nu^{(\mathrm{WKB})}=\lim_{r\to\infty}[w_\nu(r)-w_\nu^{(c)}(r)] . \tag{3.19}$$

It is important to make two observations about the above equation since it is a key result of this paper. First, it is easy to show that, if $U(r)$ has the form of a short-range potential plus a Coulomb part, then the WKB non-Coulomb phase shift approaches a finite limit as $r\to\infty$. Second, this form for the WKB non-Coulomb phase shift holds, not only for $E>0$, but also for $E<0$. When $E<0$, $\delta_\nu^{(\mathrm{WKB})}$ acquires an imaginary part since the integration in the term $w_\nu(r)$ begins at the smaller turning point. This equation for the phase shift will be used in satisfying the boundary conditions for the regular and irregular parts of the radial Green's function.

D. WKB bound states

The WKB solutions for bound states are well known. We present them here to show the Green's function will have resonances at the WKB bound-state energy levels and for the sake of completeness. Imposing the condition that the bound states must vanish at $r=0$ and ∞, as well as the normalization condition, we can determine all of the unknown constants and also the WKB energy levels given by the condition

$$\alpha_\nu=\int_{r_0}^{r_1}C_\nu(r')dr'=(n'+\tfrac{1}{2})\pi=(n-l-\tfrac{1}{2})\pi . \tag{3.20}$$

Here, n' is the radial quantum number which counts the number of nodes in the radial wave function excluding those at $r=0$ and ∞. The quantum numbers n and l are the usual principal and angular momentum quantum numbers. The values of the constants for the WKB bound-state solutions are given in Table I.

E. Regular and irregular parts of the radial Green's function

The procedure for evaluating the constants contained in the general WKB solutions for the radial Green's function is to impose all boundary conditions which do not involve the asymptotic behavior of the solution as $r\sim\infty$, and then match the asymptotic form of the general WKB solution with the required form.

For the regular part of the Green's function, the regularity condition together with Eqs. (3.8) and (3.9) allow us to write all ten constants in the general solution in terms of two of them so that the solution in region *III* has the following form:

$$R_\nu^{(III)}(r)=(2/\pi)^{1/2}|C_\nu(r)|^{-1/2} \times\{-A'_{III}\exp[+|w'_\nu(r)|] +B'_{III}\exp[-|w'_\nu(r)|]\} , \tag{3.21}$$

where we have introduced two constants A'_{III} and B'_{III} defined by

$$A'_{III}=-2A\cos(\alpha_\nu)\cos(\pi/6) , \tag{3.22a}$$

$$B'_{III}=B_{III}(2/\pi)^{-1/2} . \tag{3.22b}$$

TABLE I. These tables present the coefficients for the WKB approximate final-state radial wave function, regular and irregular parts of the Green's function, and the radial bound-state wave function. They are used in conjunction with Eqs. (3.25) and (3.26). The constant N in the bound-state wave-function coefficients is determined by normalization. In practice, this is done numerically.

	A_I	B_I	A	B
u_{ν_N}	$\frac{1}{2}\left[\frac{2}{\pi}\right]^{1/2}$	0	$\frac{1}{2\cos\left[\frac{\pi}{6}\right]}$	$\frac{1}{2\cos\left[\frac{\pi}{6}\right]}$
u_{ν_0}	$\frac{1}{N}\left[\frac{2}{\pi}\right]^{1/2}\cos\left[\frac{\pi}{6}\right]$	0	$\frac{1}{N}$	$\frac{1}{N}$
R_ν	$\frac{\left[\frac{2}{\pi}\right]^{1/2} e^{-i(\alpha_\nu-\sigma_\nu)}}{4\cos(\alpha_\nu)}$	0	$\frac{e^{-i(\alpha_\nu-\sigma_\nu)}}{4\cos(\alpha_\nu)\cos\left[\frac{\pi}{6}\right]}$	$\frac{e^{-i(\alpha_\nu-\sigma_\nu)}}{4\cos(\alpha_\nu)\cos\left[\frac{\pi}{6}\right]}$
I_ν	0	$\left[\frac{2}{\pi}\right]^{1/2} e^{i(\alpha_\nu-\sigma_\nu)}\cos(\alpha_\nu)$	$\frac{e^{i(\alpha_\nu-\sigma_\nu)}\sin\left[\alpha_\nu-\frac{\pi}{3}\right]}{\cos\left[\frac{\pi}{6}\right]}$	$\frac{-e^{i(\alpha_\nu-\sigma_\nu)}\sin\left[\alpha_\nu-\frac{2\pi}{3}\right]}{\cos\left[\frac{\pi}{6}\right]}$

	A_{II}	B_{II}	A'	B'
u_{ν_N}	$\frac{1}{2}\left[\frac{2}{\pi}\right]^{1/2} e^{-i\pi/4}$	$\frac{1}{2}\left[\frac{2}{\pi}\right]^{1/2} e^{+i\pi/4}$		
u_{ν_0}	$\frac{1}{N}\left[\frac{2}{\pi}\right]^{1/2} e^{-i\pi/4}\cos\left[\frac{\pi}{6}\right]$	$\frac{1}{N}\left[\frac{2}{\pi}\right]^{1/2} e^{+i\pi/4}\cos\left[\frac{\pi}{6}\right]$	$\frac{(-1)^{n-l-1}}{N}$	$\frac{(-1)^{n-l-1}}{N}$
R_ν	$\frac{\left[\frac{2}{\pi}\right]^{1/2} e^{-i(\alpha_\nu-\sigma_\nu)}}{4\cos(\alpha_\nu)} e^{-i\pi/4}$	$\frac{\left[\frac{2}{\pi}\right]^{1/2} e^{-i(\alpha_\nu-\sigma_\nu)}}{4\cos(\alpha_\nu)} e^{+i\pi/4}$	$\frac{e^{-i(\alpha_\nu-\sigma_\nu)}\sin\left[\alpha_\nu-\frac{\pi}{3}\right]}{2\cos(\alpha_\nu)\cos\left[\frac{\pi}{6}\right]}$	$\frac{-e^{-i(\alpha_\nu-\sigma_\nu)}\sin\left[\alpha_\nu-\frac{2\pi}{3}\right]}{2\cos(\alpha_\nu)\cos\left[\frac{\pi}{6}\right]}$
I_ν	$\frac{1}{2}\left[\frac{2}{\pi}\right]^{1/2} e^{i(\alpha_\nu-\sigma_\nu)} e^{-i(\alpha_\nu-\pi/4)}$	$\frac{1}{2}\left[\frac{2}{\pi}\right]^{1/2} e^{i(\alpha_\nu-\sigma_\nu)} e^{+i(\alpha_\nu-\pi/4)}$	$\frac{e^{i(\alpha_\nu-\sigma_\nu)}}{2\cos\left[\frac{\pi}{6}\right]}$	$\frac{e^{i(\alpha_\nu-\sigma_\nu)}}{2\cos\left[\frac{\pi}{6}\right]}$

	A_{III}	B_{III}
u_{ν_N}		
u_{ν_0}	0	$\frac{(-1)^{n-l-1}}{N}\left[\frac{2}{\pi}\right]^{1/2}\cos\left[\frac{\pi}{6}\right]$
R_ν	$\frac{1}{2}\left[\frac{2}{\pi}\right]^{1/2} e^{-i\pi/4} e^{-i(\alpha_\nu-\sigma_\nu-\pi/4)}$	$\frac{1}{2}\left[\frac{2}{\pi}\right]^{1/2} e^{-i\pi/4} e^{+i(\alpha_\nu-\sigma_\nu-\pi/4)}$
I_ν	0	$\frac{1}{2}\left[\frac{2}{\pi}\right]^{1/2} e^{i(\alpha_\nu-\sigma_\nu)}$

These constants are more convenient for matching the asymptotic forms of $R_\nu(r)$ [Eqs. (2.7)] and $R_\nu^{(III)}(r)$. For $E<0$, we can write the asymptotic form of $R_\nu^{(III)}(r)$ as follows:

$$R_\nu^{(III)} \underset{r\sim\infty}{\sim} (2/\pi)^{1/2}|k|^{-1/2}D \times\sin[kr-\tfrac{1}{2}l\pi+(1/k)ln\,(2kr) +\beta'_\nu+\sigma_\nu+\delta_\nu^{(\mathrm{WKB})}], \tag{3.23a}$$

where we have put

$$A'_{III}=-D\exp[-i(\beta'_\nu+\alpha_\nu+\pi/4)]/(2i)\ , \tag{3.23b}$$

$$B'_{III}=D\exp[i(\beta'_\nu+\alpha_\nu+\pi/4)]/(2i)\ , \tag{3.23c}$$

σ_ν is

$$\sigma_\nu=\lim_{r\to\infty}\{w_\nu^{(c)}(r)+\pi/4-[kr-\tfrac{1}{2}l\pi+(1/k)\ln(2kr)]\}\ , \tag{3.23d}$$

and we have used the relation $w_\nu(r)+w'_\nu(r)=\alpha_\nu$ for $r>r_0$. Comparing Eq. (3.23a) with Eq. (2.7b) yields

$$D=e^{-i\pi/4}\ , \tag{3.24a}$$

$$\beta'_\nu=\eta_\nu-\sigma_\nu\ . \tag{3.24b}$$

Note that since only below-threshold processes are considered in this paper, $E<0$ for the Green's functions and therefore $\eta_\nu=0$ here.

These constants are chosen so that, in the limit where the non-Coulomb part of the electronic potential vanishes, the asymptotic form of the regular part of $R_\nu^{(III)}(r)$ agrees with that for $R_\nu(r)$ in the hydrogenic case. Also the WKB non-Coulomb phase shift is again given by Eq. (3.19). Comparing Eqs. (3.21) and (3.24), the constants A'_{III}) and B'_{III} can be evaluated and therefore so can all of the constants needed for a complete determination of the regular part of the WKB radial Green's function.

To determine the constants for the irregular part we first apply the irregularity condition at the origin. It is easy to show that Eq. (3.6a) has the correct asymptotic behavior for small r if A_I is set to zero in the WKB general solution. Also, by Eq. (2.8b), the irregular Green's function decays to zero for large r, thus we set A_{III} equal to zero. The constant B_{III} is then determined by the same method as for the regular part of the WKB Green's function. With these conditions along with Eqs. (3.8) and (3.9) all of the ten constants may be evaluated.

F. The final WKB solutions

All of the wave functions and the regular and irregular parts of the Green's function are now determined under the WKB approximation. Their complete definition may be found in Table I. This table lists the constants A_I, B_I, A, B, A_{II}, B_{II}, A', B', A_{III}, and B_{III} for the four functions $u_{\nu_N}(r)$, $u_{\nu_0}(r)$, $R_\nu(r)$, and $I_\nu(r)$.

The constants in Table I correspond to those in the following transformed WKB solutions.

For $E>0$,

$$\psi_\nu^{(I)}(r)=|C_\nu(r)|^{-1/2}\{A_I\exp[-|w_\nu(r)|] +B_I\exp[+|w_\nu(r)|]\}\ , \tag{3.25a}$$

$$\psi_\nu^{(A)}(r)=[w_\nu(r)/C_\nu(r)]^{1/2}[AJ_{+1/3}(w_\nu(r)) +BJ_{-1/3}(w_\nu(r))]\ , \tag{3.25b}$$

$$\psi_\nu^{(II)}(r)=[C_\nu(r)]^{-1/2}\{A_{II}\exp[iw_\nu(r)] +B_{II}\exp[-iw_\nu(r)]\}\ , \tag{3.25c}$$

where $C_\nu(r)$ and $w_\nu(r)$ are defined in Eqs. (3.11a) and (3.11b), respectively.

For $E<0$,

$$\psi_\nu^{(I)}(r)=|C_\nu(r)|^{-1/2}\{A_I\exp[-|w_\nu(r)|] +B_I\exp[+|w_\nu(r)|]\}, \tag{3.26a}$$

$$\psi_\nu^{(A)}(r)=[w_\nu(r)/C_\nu(r)]^{1/2}[AJ_{+1/3}(w_\nu(r)) +BJ_{-1/3}(w_\nu(r))]\ , \tag{3.26b}$$

$$\psi_\nu^{(II)}(r)=[C_\nu(r)]^{-1/2}\{A_{II}\exp[+iw_\nu(r)] +B_{II}\exp[-iw_\nu(r)]\}\ , \tag{3.26c}$$

$$\psi_\nu^{(B)}(r)=[w'_\nu(r)/C_\nu(r)]^{1/2}[A'J_{+1/3}(w'_\nu(r)) +B'J_{-1/3}(w'_\nu(r))]\ , \tag{3.26d}$$

$$\psi_\nu^{(III)}(r)=|C_\nu(r)|^{-1/2}\{A_{III}\exp[+|w'_\nu(r)|] +B_{III}\exp[-|w'_\nu(r)|]\}\ , \tag{3.26e}$$

and $w'_\nu(r)$ is defined in Eq. (3.11c).

In computing the quantities $C_\nu(r)$, $w_\nu(r)$, and $w'_\nu(r)$ it is critical to take the proper branch of the complex square root of $C_\nu^2(r)$. Since $C_\nu^2(r)$ is always a real number, $|C_\nu(r)|$ is the positive real square root of $|C_\nu^2(r)|$. Then, for $E>0$,

$$C_\nu(r)=\begin{cases} i|C_\nu(r)|, & r<r_0 \\ |C_\nu(r)|, & r>r_0 \end{cases} \tag{3.27a}$$

and for $E<0$,

$$C_\nu(r)=\begin{cases} i|C_\nu(r)|, & r<r_0 \\ |C_\nu(r)|, & r_0<r<r_1 \\ i|C_\nu(r)|, & r>r_1. \end{cases} \tag{3.27b}$$

For the integrals $w_\nu(r)$ and $w'_\nu(r)$ we have, for $E<0$ and $E>0$,

$$w_\nu(r)=\begin{cases} -i\int_r^{r_0}|C_\nu(r')|dr', & r<r_0 \\ \int_{r_0}^{r}|C_\nu(r')|dr', & r>r_0 \end{cases} \tag{3.28a}$$

and

$$w'_\nu(r)=\begin{cases} \int_r^{r_1}|C_\nu(r')|dr', & r<r_1 \\ -i\int_{r_1}^{r}|C_\nu(r')|dr', & r>r_1\ . \end{cases} \tag{3.28b}$$

The integral $w'_\nu(r)$ is only used when $E<0$.

IV. REGIONS OF VALIDITY OF PROPER AND LOCAL WKB SOLUTIONS

The exact locations of the end points of regions A and B around the turning points must be determined in order to smoothly connect the solutions. These end points are determined by the well-known [9] condition for validity of the proper WKB solutions. This condition [in terms of $x=\ln(r/a_0)=\ln(r)$, because $a_0=1$ a.u.] is

$$|f(x)| \ll 1 , \tag{4.1}$$

where

$$f(x)=\frac{2[E-U_{\text{eff}}(x)]-U'_{\text{eff}}(x)}{\{2[E-U_{\text{eff}}(x)]\}^{3/2}} , \tag{4.2}$$

and where $U'_{\text{eff}}(x)$ denotes the derivative of $U_{\text{eff}}(x)$ with respect to x. A tolerance (ϵ) is specified and the proper solution appropriate to the value of r is used whenever

$$|f(x)| < \epsilon , \tag{4.3}$$

otherwise the appropriate local solution is used. In the calculation of H and Cs cross sections a tolerance of $\epsilon=0.1$ was used.

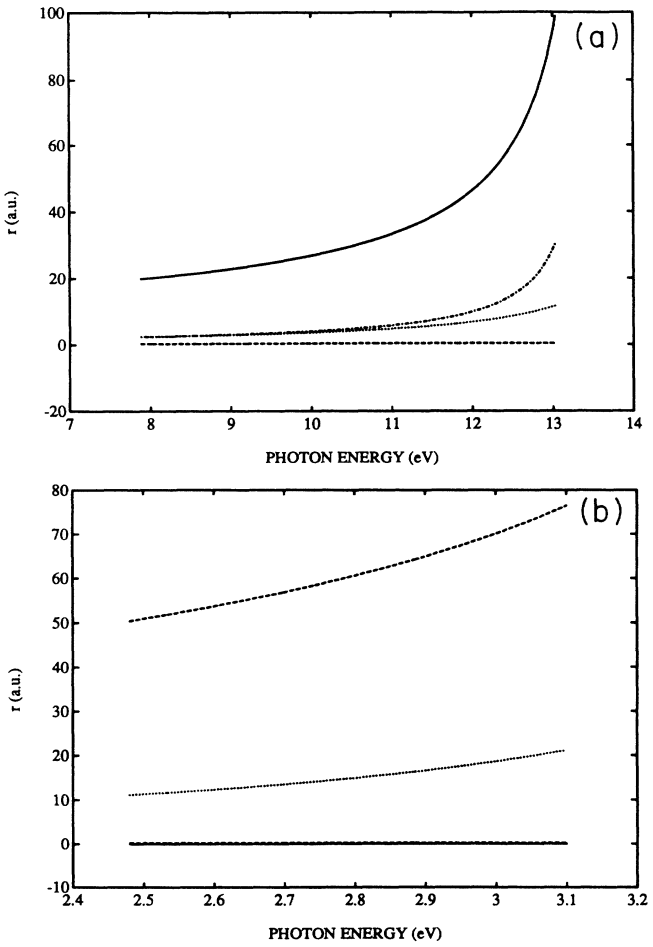

FIG. 2. (a) A plot of the solution of $|f(r)|=0.1$ as a function of photon energy for hydrogen with $l=1$. The dashed curve represents the boundary between regions I and A, the dotted curve is the boundary between regions A and II, the dash-dotted curve is the boundary between regions II and B, and the solid curve is the boundary between regions B and III. The vertical axis represents the radial electron coordinate and negative values are shown so that the lowest curve can be distinguished from the $r=0$ line. (b) A similar plot for Cs with $l=1$. The lowest curve is actually two curves which cannot be distinguished on the scale of the graph.

For $E<0$, the validity function exhibits two divergent peaks at the locations of the turning points. The local solution provides a good approximation to the exact solution in regions close to a turning point and also far from a turning point. At intermediate distances, the approximation is less good. Thus, for optimum performance of this method, the separation of the turning points should be large compared to the size of the regions in which the local solutions are valid. If this is only marginally the case "glitches" appear in the graph of the WKB approximate wave function.

Figure 2(a) shows the regions I, A, II, B, and III for the WKB hydrogenic Green's function as a function of photon energy. For a given photon energy (horizontal axis), the lowest (dashed) of the four curves represents the boundary between region I and region A. The second lowest (dotted) curve represents the boundary between region A and region II, the next (dash-dotted) curve represents the boundary between regions II and B, and the highest (solid) curve is the boundary between regions B and III. The vertical axis is the radial coordinate and negative values are shown so that the lowest curve can be distinguished from the $r=0$ line. These curves are the solutions of $|f(x)|=\epsilon$ (where $\epsilon=0.1$ to match the case of the cross section curve presented later).

Note that region II [between the middle two curves in Fig. 2(a)] is always much smaller than region B (between the upper two curves). This indicates that the approximation of "well-spaced" turning points is marginal for hydrogen. This does not radically affect the accuracy of the calculated cross sections as will be seen in Sec. V. It is also possible to treat the case of "closely spaced" turning points [9].

Although it may seem inappropriate to use a "local solution" in the rather large region B, we emphasize here that these solutions satisfy the differential equation in the neighborhood of the turning points and also at large distances away from them. Thus, at large distances from the turning points, the difference between the proper solution and the local solution is negligible. This provides for a smooth transition from local to proper solution at the end point of the local region. It also indicates that there may be a better criterion for deciding which solution to use other than the traditional WKB validity function.

The corresponding validity region plot for Cs is shown in Fig. 2(b). Here the lowest curve is actually two curves which are so close together on the scale of the graph that they coalesce. This indicates that regions I and A are extremely small compared to regions II and B. The well-spaced turning point approximation is therefore much better for Cs than for H.

V. TWO-PHOTON IONIZATION OF HYDROGEN AND CESIUM

To assess the performance of this method we have calculated the cross section for two-photon ionization of hydrogen and cesium with linearly polarized light. The two-photon radial matrix elements [Eq. (2.1)] were calculated by a method similar to that of Ref. [7] which we briefly recount here.

For linearly polarized light, the two-photon-ionization cross section can be written as

$$\sigma_2^{(L)}=(8.069\times10^{-53})E_{\rm ph}^2\tfrac{1}{9}(|M^{(2)}_{\nu_{20}\nu_1\nu_0}|^2+\tfrac{4}{5}|M^{(2)}_{\nu_{22}\nu_1\nu_0}|^2)\ , \tag{5.1}$$

where $M^{(2)}_{\nu_{20}\nu_1\nu_0}$, $M^{(2)}_{\nu_{22}\nu_1\nu_0}$, and $E_{\rm ph}$ are expressed in atomic units, $\sigma_2^{(L)}$ is expressed in cm^4 sec, and

$$\nu_0=(E_0,l_0)=(-E_{\rm ion},0)\ , \tag{5.2a}$$

$$\nu_1=(E_1,l_1)=(-E_{\rm ion}+E_{\rm ph},1)\ , \tag{5.2b}$$

$$\nu_{22}=(E_2,l_{22})=(-E_{\rm ion}+2E_{\rm ph},2)\ , \tag{5.2c}$$

$$\nu_{20}=(E_2,l_{20})=(-E_{\rm ion}+2E_{\rm ph},0)\ , \tag{5.2d}$$

where $E_{\rm ion}$ is the ionization energy of the atom in atomic units.

The double integral over all values of r_1 and r_2 represented by $M^{(2)}_{\nu_2\nu_1\nu_0}$ is split into two integrals. One of these has as its region of integration that part of the r_1r_2 plane for which $r_1>r_2$ and the other that for which $r_2>r_1$. Inside these regions the $r_>$ and $r_<$ coordinates may be explicitly assigned. We then choose to perform each of these double integrals in an order such that the inner integral is over the smaller coordinate. Thus $M^{(2)}_{\nu_2\nu_1\nu_0}$ may be expressed as

$$(-1/2\pi)M^{(2)}_{\nu_2\nu_1\nu_0}=\int_0^\infty dr_2 u_{\nu_2}(r_2)r_2 I_{\nu_1}(r_2)\int_0^{r_2}dr_1 R_{\nu_1}(r_1)r_1 u_{\nu_0}(r_1)+\int_0^\infty dr_1 I_{\nu_1}(r_1)r_1 u_{\nu_0}(r_1)\int_0^{r_1}dr_2 u_{\nu_2}(r_2)r_2 R_{\nu_1}(r_2)\ . \tag{5.3}$$

Each of these integrals can be converted into a system of first-order differential equations. The differential systems were evaluated with a fourth-order Runge-Kutta algorithm. In contrast to the method in Ref. [7], however, no rotation of the integration contour into the complex plane was performed.

The calculated hydrogenic cross sections are presented in Table II and also in Fig. 3(a). Table II shows a quantitative comparison of hydrogenic cross sections from the present work with those calculated by Karule [10]. The differences range from less than 1% to just larger than a factor of 2. Figure 3(a) contains a graph of the hydrogenic cross section as a function of the photon energy. The resonances are in the correct positions. This is not surprising because the regular part of the WKB Green's function depends inversely on $\cos(\alpha_\nu)$ and, for resonant photon energies, α_ν equals a half-integral multiple of π. Thus, since the WKB approximation produces exact energy-level positions for H, the resonances in the WKB Green's function will be correctly positioned. This point

TABLE II. A comparison of WKB hydrogenic two-photon-ionization cross sections using linearly polarized laser light with the exact cross sections of Ref. [10]. The quantities in square brackets indicate the power of 10 by which the number preceding the brackets is multiplied.

Photon wavelength (Å)	Present work (cm^4 sec)	Ref. [10] (cm^4 sec)
1700	1.247[−50]	1.203[−50]
1600	1.159[−50]	1.136[−50]
1400	1.191[−50]	1.199[−50]
1300	2.091[−50]	1.940[−50]
1200	1.257[−49]	1.063[−49]
1100	1.609[−51]	7.223[−52]
1020	5.103[−51]	1.381[−50]

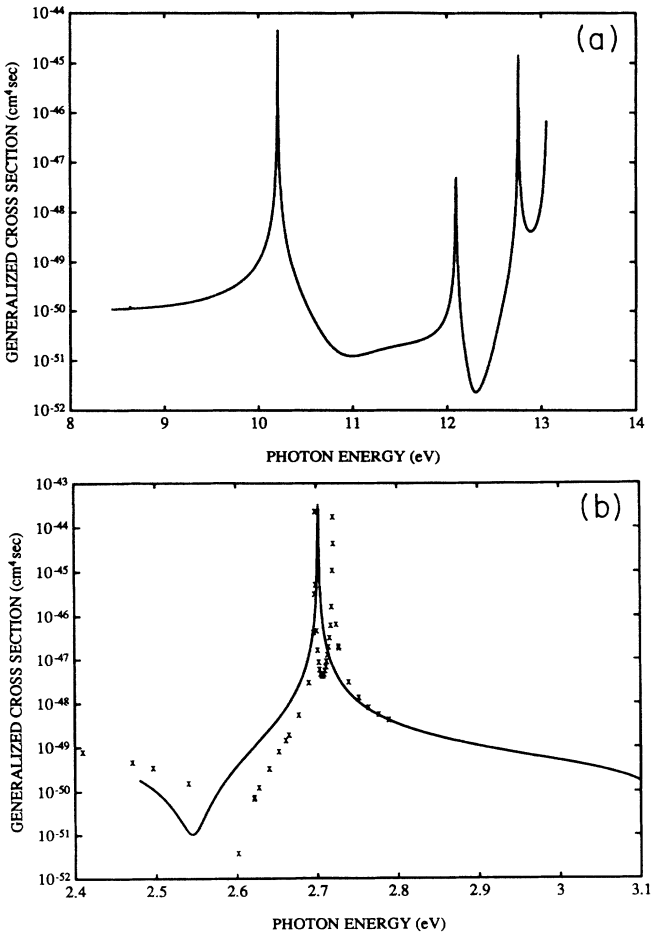

FIG. 3. (a) A plot of the two-photon-ionization cross section of H vs photon energy. (b) A similar plot for Cs around the $7p$ resonance. The points marked with an "×" are the results of Ref. [14].

is critical in choosing the potential for Cs which is optimal for this method.

We have chosen to calculate Cs cross sections around the $7p$ resonance as a first test of this method for two reasons. First, it is one of the few cases for which there exist measurements of absolute cross sections [11]. Second, a large body of careful theoretical work exists for this case [12–14]. Especially useful is the calculation of Ref. [14] whose results are in tabular rather than graphical form allowing a careful comparison with the present work. Figure 3(b) contains a graph of the two-photon-ionization cross section of Cs with linearly polarized light for photon energies ranging from 2.5 to 3.1 eV. This range scans across the $7p$ resonance. The points marked with an "×" are the data of Ref. [14]. The agreement is reasonable considering the fact that the calculation of Ref. [14] included spin-orbit effects and the present work did not (note that the cross section data of Ref. [14] exhibit two resonances, the $7p_{1/2}$ and $7p_{3/2}$). It is worth noting that the experimental position of the antiresonance falls at approximately 2.58 eV, which is between that of this work and that of Ref. [14].

The cross sections in this work were calculated using a SUN SparcStation 2-GS. Each cross section required approximately 5 min on this machine. One numerical advantage of this method is that about the same amount of computing time is required for Cs as for H. The only difference in the computer program is the atomic potential.

The most critical element required for the success of this method is choosing the optimal atomic potential. The potential chosen for Cs and the criterion for choosing it will be discussed in the following section.

VI. DISCUSSION: CHOOSING THE ATOMIC POTENTIAL

In deciding what form to use for the potential for Cs we were guided by the simple argument of the preceding section regarding the positions of the hydrogenic cross-section resonances. For hydrogen, the exact potential is known, and it is a fortuitous circumstance that the WKB energy levels for H are equal to the exact ones. It is clear that, if the WKB approximate energies had been different from the exact ones, the cross-section results would have been very poor because the resonances would have been out of position.

We chose the Cs atomic potential such that the WKB energy levels for this potential agree with the experimental levels. The form of the potential used in the present work follows an analytical form used previously in connection with the Thomas-Fermi potential [15]. We present here the electronic potential energy [the quantity $U(r)$ in Eq. 3.11(a)]

$$U(r)=-(1/r)[(Z-1)\phi(r/\mu)+1]\ , \tag{6.1a}$$

TABLE III. A list of the values of the parameters α_k used in the model potential for Cs [Eqs. (6.1)].

k	α_k
1	−0.555 802
2	+2.898 796
3	−2.077 431
4	+0.338 513
5	+0.363 840
6	−0.011 988

where

$$\phi(y)=\left[1+\sum_{k=1}^{6}\alpha_k y^{k/2}\right]^{-1} \tag{6.1b}$$

and

$$\mu=0.8853Z^{-1/3}\ .$$

The symbol Z is the atomic number.

The six parameters α_k were determined so that the WKB energy levels, as determined by Eq. (3.20), matched the $6s$, $7p_{1/2}$, $8p_{1/2}$, $9p_{1/2}$, $10p_{1/2}$, and $11p_{1/2}$ experimental levels [16]. We also note that it is crucial that one of the fitted energy levels be the ground state. The values of these parameters are listed in Table III. How these values were obtained and values of the α_k for other atoms will be subject of a forthcoming article.

The idea of using the experimental energy levels to determine the form of the potential is not new [17]; in fact it is quite old, but it is certainly different in this context. It is also possible to include spin-orbit effects in this technique.

In conclusion, we have presented a method for uniformly approximating all of the functions which appear in the N-photon radial matrix element using the WKB approximation. Furthermore, we have calculated cross sections for two-photon ionization of H and Cs ionized by linearly polarized light and compared the results with other work.

This method can also be applied to the calculation of other useful quantities such as atomic parameters used in effective Hamiltonian calculations and optical parameters of gases such as indexes of refraction. More work, however, is needed on the determination of the best potential to use, on the refinement of the WKB validity criterion, on the inclusion of spin-orbit effects, and on further testing with other atoms.

ACKNOWLEDGMENTS

It is a pleasure to thank Dr. R. M. Steinman for providing computer support under AFOSR Grant No. 91-0124.

[1] See, e.g., T. J. McIlrath, P. H. Bucksbaum, R. R. Freeman, and M. Bashkansky, Phys. Rev. A **35**, 4611 (1987).
[2] P. Lambropoulos, Adv. At. Mol. Phys. **12**, 87 (1976).
[3] A. Dalgarno and J. T. Lewis, Proc. R. Soc. London **233**, 70 (1955); M. Aymar and M. Crance, J. Phys. B **14**, 3585 (1981).
[4] See, M. Crance, in *Multiphoton Ionization of Atoms,* edited by S. L. Chin and P. Lambropoulos (Academic, Toronto, 1984).
[5] A. L'Huillier, X. Tang, and P. Lambropoulos, Phys. Rev. A **39**, 1112 (1989).
[6] X. Tang, T. N. Chang, P. Lambropoulos, S. Fournier, and L. F. DiMauro, Phys. Rev. A **41**, 5265 (1990).
[7] M. Edwards, X. Tang, and R. Shakeshaft, Phys. Rev. A **35**, 3578 (1987).
[8] R. Langer, Phys. Rev. A **51**, 669 (1937).
[9] See, e.g, P.M. Morse and H. Feshbach, *Methods of Theoretical Physics* (McGraw-Hill, New York, 1953).
[10] E. Karule, J. Phys. B **11**, 441 (1978).
[11] J. Morellec, D. Normand, G. Mainfray, and C. Manus, Phys. Rev. Lett. **44**, 1394 (1980).
[12] H. B. Bebb, Phys. Rev. **153**, 23 (1967).
[13] A. Rachman, G. Laplanche, and M. Jaouen, Phys. Lett. **68A**, 433 (1978).
[14] M. R. Teague, P. Lambropoulos, D. Goodmanson, and D. W. Norcross, Phys. Rev. A **14**, 1057 (1976).
[15] R. Latter, Phys. Rev. **99**, 510 (1955).
[16] C. E. Moore, *Atomic Energy Levels,* Natl. Bur. Stand. (U.S.) Circ. No. 467 (U.S. GPO, Washington DC, 1958), Vol. III.
[17] E. U. Condon and G. H. Shortley, *The Theory of Atomic Spectra* (Cambridge University Press, Cambridge, England, 1963).